Rlp7p is associated with 60S preribosomes, restricted to the granular component of the nucleolus, and required for pre-rRNA processing

JCB Article

Rlp7p is associated with 60S preribosomes, restricted to the granular component of the nucleolus, and required for pre-rRNA processing

Olivier Gadal,[1] Daniela Strauss,[1] Elisabeth Petfalski,[2] Pierre-Emmanuel Gleizes,[3] Nicole Gas,[3] David Tollervey,[2] and Ed Hurt[1]

[1]BZH, Biochemie-Zentrum Heidelberg, D-69120 Heidelberg, Germany
[2]Wellcome Trust Centre for Cell Biology, University of Edinburgh, Swann Building, Edinburgh EH9 3JR, UK
[3]Laboratoire de Biologie Moleculaire Eucaryote, F-32062 Toulouse, France

Many analyses have examined subnucleolar structures in eukaryotic cells, but the relationship between morphological structures, pre-rRNA processing, and ribosomal particle assembly has remained unclear. Using a visual assay for export of the 60S ribosomal subunit, we isolated a ts-lethal mutation, *rix9-1*, which causes nucleolar accumulation of an Rpl25p-eGFP reporter construct. The mutation results in a single amino acid substitution ($F_{176}S$) in Rlp7p, an essential nucleolar protein related to ribosomal protein Rpl7p. The *rix9-1* (*rlp7-1*) mutation blocks the late pre-RNA cleavage at site C_2 in ITS2, which separates the precursors to the 5.8S and 25S rRNAs. Consistent with this, synthesis of the mature 5.8S and 25S rRNAs was blocked in the *rlp7-1* strain at nonpermissive temperature, whereas 18S rRNA synthesis continued. Moreover, pre-rRNA containing ITS2 accumulates in the nucleolus of *rix9-1* cells as revealed by in situ hybridization. Finally, tagged Rlp7p was shown to associate with a pre-60S particle, and fluorescence microscopy and immuno-EM localized Rlp7p to a subregion of the nucleolus, which could be the granular component (GC). All together, these data suggest that pre-rRNA cleavage at site C_2 specifically requires Rlp7p and occurs within pre-60S particles located in the GC region of the nucleolus.

Introduction

In *Saccharomyces cerevisiae*, ribosome biogenesis is one of the most energy-consuming processes in the cell. rRNA transcription represents >60% of the total transcription (Warner, 1999). Two pre-rRNAs are produced, the pre-5S rRNA transcribed by RNA polymerase III, and a large RNA polymerase I transcript (35S pre-rRNA in yeast). Ribosomal proteins are synthesized in the cytoplasm and actively imported into the nucleus, where they associate with newly transcribed pre-rRNAs to generate preribosomal particles (Woolford, 1991). These precursor particles are large ribonucleoprotein complexes in which the rRNAs undergo nucleotide modification at many positions and are processed at multiple sites to generate the 25S/28S, 18S, and 5.8S rRNAs present in the mature ribosomes (Kressler et al., 1999).

Most steps in ribosome synthesis occur in the nucleolus, a specialized nuclear compartment. The nucleolus is a highly dynamic structure, and three subregions, fibrillar centers (FCs),* a dense fibrillar component (DFC), and a granular component (GC), can be distinguished in chemically fixed samples of many cells (for review see Shaw and Jordan, 1995; Scheer and Hock, 1999). Using these conventional methods of preparing samples, the ultrastructure of yeast nucleolus cannot be preserved, and it was described as dense crescent into the nucleus (Sillevis-Smitt et al., 1973). However, cryofixation and cryosubstitution can optimally preserve the cellular ultrastructure, allowing the three subnucleolar compartments to be observed in *S. cerevisiae* (Léger-Silvestre et al., 1999).

The relationship between the observed subnucleolar structures and the different steps of ribosome biogenesis is not well established and remains somewhat controversial (for review

Address correspondence to Eduard Hurt, Biochemie-Zentrum Heidelberg (BZH), Im Neuenheimer Feld 328, D-69120 Heidelberg, Germany. Tel.: 49-6221-54-4173. Fax: 49-6221-54-4369.
E-mail: cg5@ix.urz.uni-heidelberg.de

O. Gadal's present address is Institute Pasteur, 25-28, Rue du Docteur Roux, 75724 Paris Cedex 15, France.

Key words: rRNA processing; ribosome biogenesis; ribosome export; nucleolus; preribosome

*Abbreviations used in this paper: DFC, dense fibrillar component; FC, fibrillar center; GC, granular component; snoRNA, small nucleolar RNA.

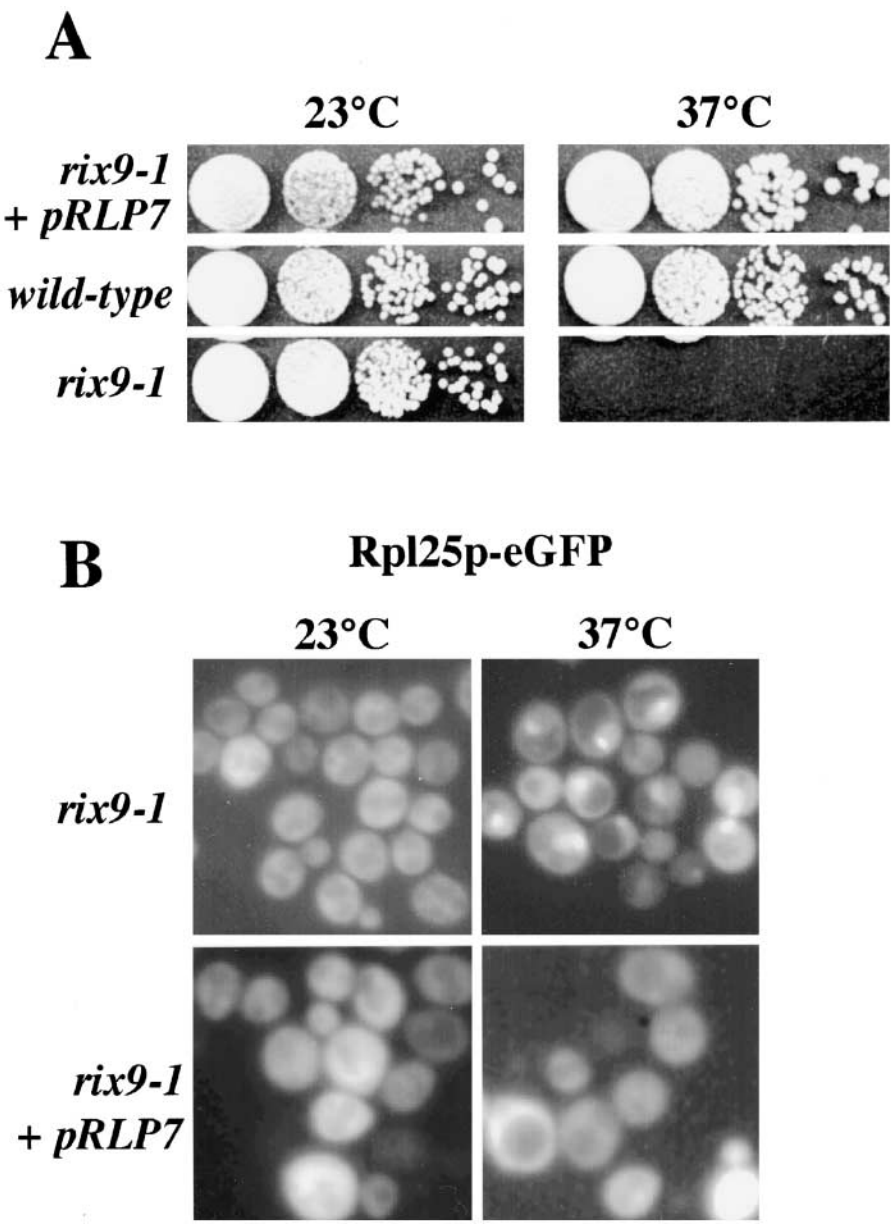

Figure 1. ***rix9-1* ts strain is complemented by *RLP7* and accumulates Rpl25p-eGFP in the nucleolus.** (A) *rix9-1* is complemented by *RLP7*. Growth properties of *rix9-1* cells, an isogenic wild-type strain, and the *rix9-1* strain harboring a plasmid containing *RLP7 (pRLP7)*. Serial dilutions of cells plated on YPD plates were incubated for 3 d at 23 or 37°C. (B) *rix9-1* cells or the *rix9-1* strain harboring a plasmid containing *RLP7 (pRLP7)* were transformed with Rpl25p-eGFP and grown at 23°C, before shift for 4 h to 37°C and inspection in the fluorescence microscope.

see Shaw and Jordan, 1995; Scheer and Hock, 1999). A plausible model is that pre-rRNA transcription occurs at the boundary between the FC and DFC. In the DFC, the pre-rRNA may assemble with the pre-rRNA processing and modification machinery, followed by small nucleolar RNA (snoRNA)-mediated rRNA modification and early processing reactions, with late processing and assembly reactions occurring in the GC. Final maturation of the subunits occurs after their release from the nucleolus and export to the cytoplasm via the nucleoplasm and nuclear pores. Many components required for the correct assembly and trafficking of the preribosomes have been identified, but how these function together in the various preribosomal particles remains unclear.

Three types of ribosomal precursor particles of different sizes were identified from yeast by sucrose gradient centrifugation (Trapman et al., 1975). The 90S preribosomal particle was reported to contain the 35S pre-rRNA (itself identified by sucrose gradient velocity) and many early-assembling ribosomal proteins. However, this size is substantially smaller than that expected for a pre-rRNA associated with the many modification guide snoRNPs, and a more recent analysis (Milkereit et al., 2001) indicates that the 35S pre-rRNA is actually found distributed in much higher weight gradient fractions. This particle is then divided into two smaller particles, presumably by cleavage of the pre-rRNA at site A_2 in ITS1 (below and see Fig. 4), generating the 66S and 43S preribosomes that are the precursors to the mature 60S and 40S subunits, respectively (Trapman et al., 1975). The 66S preribosomal particle contains the $27SA_2$, 27SB, and 7S pre-rRNA species, whereas the 43S particle contains the 20S pre-rRNA (Milkereit et al., 2001). Many nonribosomal proteins were shown to be associated with the preribosomal particles (Bassler et al., 2001; Harnpicharnchai et al., 2001; Saveanu et al., 2001). For example, the Noc1p–Noc2p and the Noc2p–Noc3p protein complexes cofractionate with the 35S and the 27S/7S pre-rRNAs, respec-

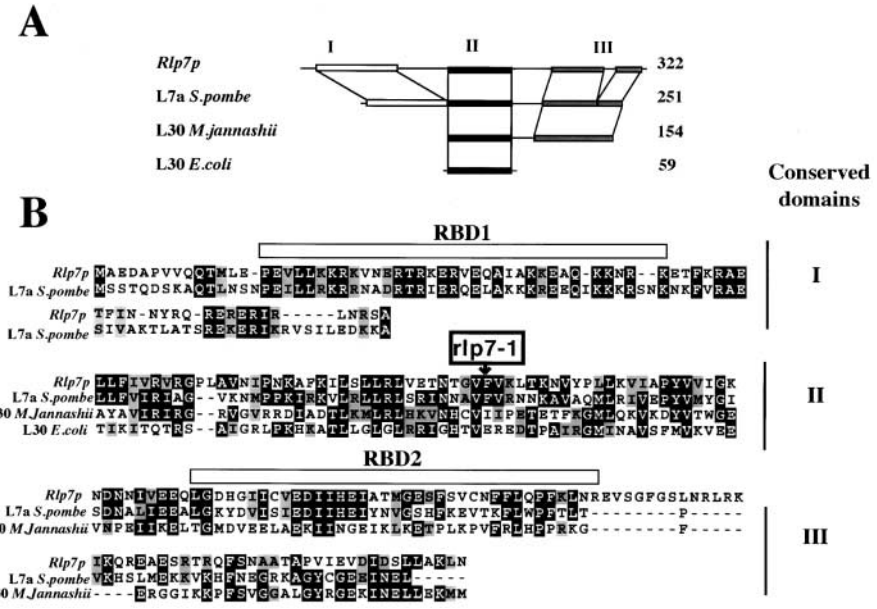

Figure 2. **Rlp7p is homologous to the ribosomal protein L7.** (A) Homology with the eukaryotic L7 is divided into three domains: domain I, exclusively eukaryotic; domain II, signature of the L30 super-family of ribosomal proteins conserved in all kingdoms of life; and domain III, present in eukaryotic and archeal proteins. (B) Multiple sequence alignment of Rlp7p with other homologues: L7a (*Schizosaccharomyces pombe*), archeal L30 (*Methanococcus jannashii*) and prokaryotic L30 (*Escherichia coli*). The two RNA-binding motifs (RBD1 and RBD2) are indicated with shaded boxes. Position of the mutation in *rlp7-1* is indicated by an arrow. Accession numbers for Rlp7p and homologues are as follows: *S. cerevisiae* (GenBank/EMBL/DDBJ accession no. Ynl002c), *S. pombe* (GenBank/EMBL/DDBJ accession no. O60143), *M. Jannashii* (GenBank/EMBL/DDBJ accession no. P54046), and *E. coli* (GenBank/EMBL/DDBJ accession no. P02430).

tively, under the extraction conditions used in this work (Milkereit et al., 2001).

Using an in vivo assay in yeast for nuclear and nucleolar retention of a fusion between a 60S subunit protein and green fluorescent protein (Rpl25p-eGFP), we identified a class of mutants impaired in 60S ribosomal subunit export (*rix*) (Gadal et al., 2001). Here we report the analysis of the *rix9-1* mutant, which showed nucleolar accumulation of the Rpl25p-eGFP reporter. The *rix9-1* strain has a single amino acid substitution in Rlp7p, which is homologous to the 60S subunit protein Rpl7p (Lalo et al., 1993). While this work was in progress, it was reported that Rlp7p is not a ribosomal protein, but an essential nucleolar protein that functions in the processing of precursors to the large ribosomal subunit rRNAs (Dunbar et al., 2000). The *rix9-1* allele shows a defect in pre-rRNA cleavage at site C_2. Rlp7p is shown to associate with 66S preribosomes and to localize to the GC subcompartment of the nucleolus. We suggest that Rlp7p has an essential function in C_2 cleavage occurring in preribosomes within the nucleolar GC.

Results

Isolation and characterization of the *rix9-1* mutant

Our screen for ribosome export defects (Gadal et al., 2001) identified *rix9-1*, which is a temperature-sensitive mutant that stops cell growth after shift to the restrictive temperature of 37°C (Fig. 1 A). The 60S subunit reporter Rpl25p-eGFP was cytoplasmic with nuclear exclusion in the *rix9-1* strain at 23°C, but accumulated in the nucleus 3 to 4 h after transfer to 37°C (Fig. 1 B). The distribution of Rpl25p-eGFP inside the nucleus was different in the various *rix* mutants, with accumulation throughout the entire nucleoplasm in some strains and predominantly nucleolar accumulation in others (Gadal et al., 2001). The *rix9-1* strains showed a predominant nucleolar accumulation of Rpl25p-eGFP at 37°C, suggesting that the release of preribosomal particles from the nucleolus to the nucleoplasm is inhibited (Fig. 1 B).

The wild-type *RIX9* gene was cloned by complementation of the ts phenotype of the *rix9-1* mutant and was shown to be identical to the gene *RLP7* (Fig. 1 A). DNA from the chromosomal locus was recovered by PCR from *rix9-1* and isogenic wild-type strains. A single nucleotide substitution was found in the *RLP7* ORF changing a conserved phenylalanine (176) to serine; therefore, this mutant was designated *rlp7-1*.

Rlp7p is strikingly homologous to the conserved ribosomal protein L7 (Rpl7p), which has close homologues in archaea and bacteria (Fig. 2 A). Three conserved domains were identified in Rpl7p homologues, with domain II best conserved. The mutation in *rlp7-1* alters a conserved residue within this domain (Fig. 2 B). Two RNA-binding domains have been mapped in human L7, designated RBD1 and RBD2 in Fig. 2 B. RBD2 is present in all homologues and binds preferentially to 28S rRNA (von Mikecz et al., 1999). These two RNA-binding domains are present in Rlp7p, and are not affected in the *rlp7-1* mutant, raising the possibility that Rlp7p binds to the same rRNA sequence as Rpl7p (see Discussion).

Rlp7p associates with preribosomes and is required for 60S ribosomal subunit biogenesis

The high degree of homology between Rlp7p and a ribosomal protein of the 60S subunit, and its apparent involvement in subunit release from the nucleolus suggested that Rlp7p might be associated with preribosomal particles. To assess this, sucrose gradient centrifugation and Western blotting was performed on a strain expressing a Protein A–tagged Rlp7p (see Materials and methods). When whole-cell lysates were fractionated, Rlp7p was detected in the fraction that contained the 60S ribosomal subunits (Fig. 3 A). We conclude that Rlp7p is associated with preribosomal particles of ~60S, presumably corresponding to the 66S preribosomes previously reported (Trapman et al., 1975).

Many strains with defects in 60S subunit biogenesis show a characteristic phenotype, with a reduced level of free 60S

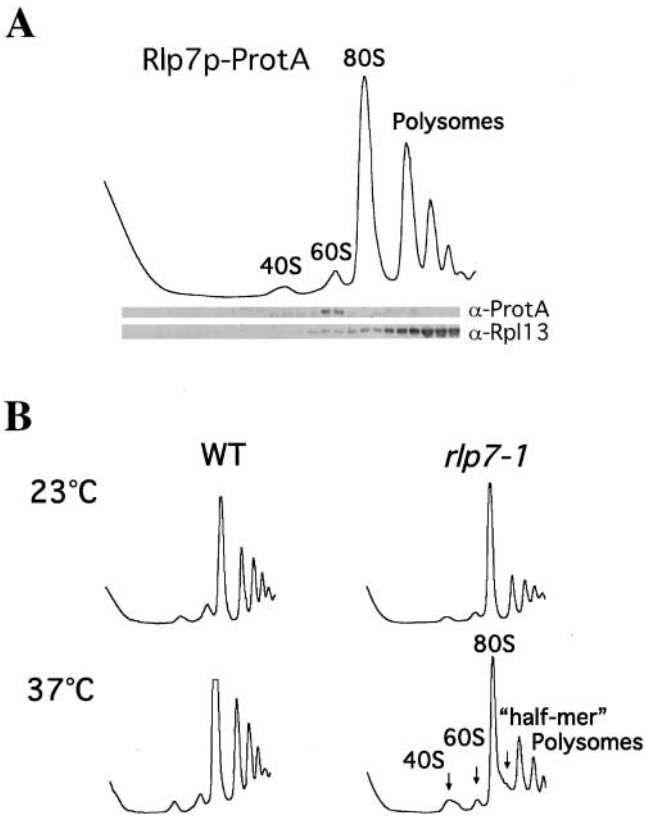

Figure 3. **Rlp7p is associated with 60S precursors and is required for 60S subunit biogenesis.** (A) Rlp7p cofractionates with 60S preribosomes. Analysis of polysomal ribosome fractions derived from cells expressing Rlp7p-ProtA. Fractions were subjected to SDS-PAGE and Western blotting using α-ProtA and α-Rpl13p antibodies. The position of 40S and 60S subunits, of 80S ribosomes, and of polysomes is indicated. (B) Polysomal profiles ($OD_{260\,nm}$) after sucrose density gradient centrifugation derived from the *rlp7-1* mutant and wild-type strain grown at permissive temperature (23°C) and 4 h after shift to restrictive temperature (37°C). The position of 40S, 60S, and 80S ribosomes, of polysomes and half-mer polysomes is indicated.

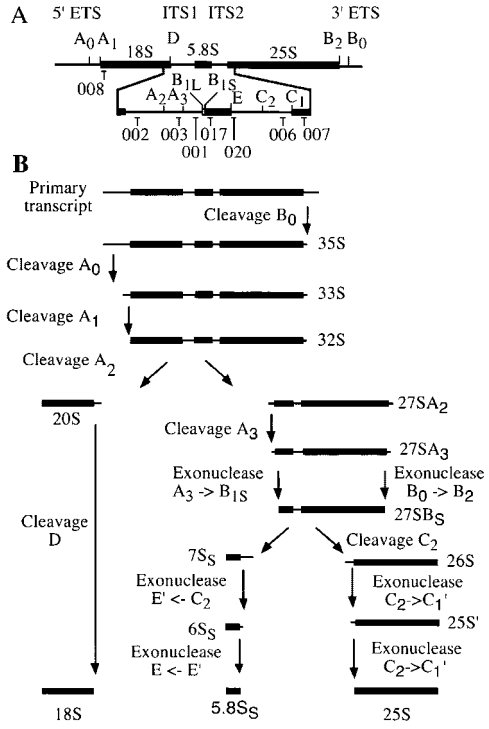

Figure 4. **Pre-rRNA structure and processing.** (A) Schematic diagram of the 35S pre-rRNA showing the processing sites and oligonucleotides used. The 35S pre-rRNA contains the sequences for the mature 18S, 5.8S, and 25S rRNAs separated by the two internal transcribed spacers, and flanked by the 5′-ETS and 3′-ETS. (B) Major pre-rRNA processing pathway.

subunits, increased free 40S, and the presence of half-mer polysomes (polysomes containing a single 40S subunit at the initiation site). To assess the involvement of Rlp7p in 60S subunit biogenesis, polysome profiles were compared for *rlp7-1* and an isogenic wild-type strain (Fig. 3 B). The polysome profile of the mutant strain was already mildly perturbed when grown at permissive temperature, with an increase in the ratio-free 40S to 60S. When *rlp7-1* cells were shifted to restrictive temperature, the amount of 60S subunits dropped further and the appearance of half-mer polysomes was noticed (Fig. 3 B). We conclude that Rlp7p is required for 60S ribosomal subunit biogenesis.

Pre-rRNA processing is defective in *rlp7-1* mutant strains

To test whether the depletion of 60S ribosomal subunits observed in the *rlp7-1* strain is a consequence of defects in pre-rRNA processing (for the structure of the pre-rRNA and processing scheme see Fig. 4), we performed Northern hybridization (Figs. 5, A and B), primer extension (Fig. 5 C), and pulse-chase analyses (Fig. 6). After transfer of the *rlp7-1* strain to 37°C for 2 h, the 35S pre-rRNA was mildly accumulated (Fig. 5 A). The $27SA_2$ and 20S pre-rRNAs were reduced, indicating that processing at sites A_1 and A_2 was partially inhibited, but there was little accumulation of the 23S RNA (the product of cleavage of 35S at site A_3 in the absence of prior cleavage at sites A_0 to A_2), which is seen in many other processing mutants. The 27SB pre-rRNA was also reduced (Fig. 5 A), and primer-extension analysis suggested that $27SB_S$ was reduced to a greater extent than $27SB_L$ (Fig. 5 C, stops at B_{1S} and B_{1L}, respectively). In the *rlp7-1* strain at 37°C, a rapid and strong reduction was seen in the levels of the 7S pre-rRNAs (Fig. 5 B) which are generated from the 27SB pre-rRNAs by cleavage at site C_2. The other product of C_2 cleavage, the 26S pre-rRNA, cannot be detected by Northern hybridization, but primer extension through site C_2 (Fig. 5 C) shows that this pre-rRNA is rapidly lost, within 2 h of transfer to 37°C. In strains depleted of a recently reported processing factor, Ssf1p, cleavage at site C_2 leads to the appearance of the A_2–C_2 fragment (Fatica et al., 2002), but this does not occur in the *rlp7-1* strain (Fig. 5 B). The 25S′ pre-rRNA, a short 5′ extended form of 25S shown by the primer extension stop at site C_1′, was strongly depleted in the *rlp7-1* strain. This is consistent with the loss of cleavage at site C_2, which acts as an entry site for the 5′ exonucleases Rat1p and Xrn1p that generate the 5′ end of 25S rRNA.

The $27SA_3$ pre-rRNA cannot be detected by Northern analysis, but its abundance is indicated by the primer exten-

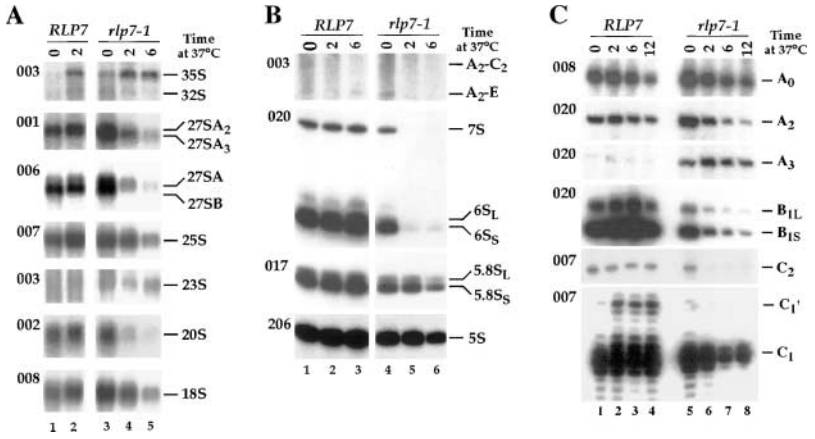

Figure 5. **Analysis of pre-rRNA processing in the *rlp7-1* strain.** (A) Northern analysis of high–molecular weight RNA separated on a 1.2% agarose/ formaldehyde gel (B) Northern analysis of low–molecular weight RNA separated on an 8% polyacrylamide/ urea gel. (C) Primer extension analysis. RNA was extracted from cells growing at 23°C (0 h samples) and after transfer to 37°C for the times indicated. Oligonucleotides used are indicated in parentheses.

sion stop at site A_3 which was strongly elevated even at the permissive temperature (Fig. 5 C). Site A_3 acts as an entry site for the Rat1p and Xrn1p exonucleases, which in this case generate the 5′ end of the $27SB_S$ pre-rRNA and $5.8S_S$ rRNA at site B_{1S}. The apparent reduction in the stop at site B_{1S} relative to B_{1L} would be consistent with reduced or delayed exonuclease processing from $27SA_3$ to 27SB.

Primer extension analysis through site A_0 showed that the 33S pre-rRNA was little affected in the *rlp7-1* strain, whereas the reduction in the stop at A_2 was consistent with the reduced level of $27SA_2$ seen in Northern analyses. Cleavage at all sites was accurate at the nucleotide level.

Pulse-chase labeling of the *rlp7-1* strain 2 h after transfer to 37°C, with either [H^3]-uracil or [H^3]-methyl methionine, showed a dramatic reduction in the synthesis of both the 25S and 5.8S rRNAs (Fig. 6). In contrast, 18S synthesis continued, but with some delay consistent with the results of Northern hybridization. The 7S pre-rRNA was not detected in the *rlp7-1* strain. Northern hybridization of the filter shown in Fig. 6 C showed that the weak band visible in the *rlp7-1* strain at the approximate position of 7S does not hybridize with a 7S pre-rRNA probe and migrates above 7S on the gel.

From these results, we conclude that the *rlp7-1* mutation leads to a delay in exonuclease processing from site A_3, together with strong inhibition of cleavage at site C_2. The delay in cleavage at sites A_0 to A_2 and 18S synthesis is a common feature of strains with defects in 60S subunit synthesis (Venema and Tollervey, 1999) and is likely to be an indirect effect.

Pre-rRNA containing ITS2 accumulates in the *rlp7-1* ts mutant

Ultrastructural detection of pre-60S ribosomal precursors by in situ hybridization was performed in wild-type and mutant *rlp7-1* cells with an ITS2-specific probe (Gleizes et al., 2001). As shown in Fig. 7, the labeling in *rlp7-1* cells at permissive temperature was found in the nucleolus, and its intensity was the same as in wild-type cells. Upon a shift to 37°C, *rlp7-1* cells displayed a strong buildup of ITS2 containing pre-rRNAs. Quantitation of these immuno-EM data (in total 30 nuclei were analyzed) yielded in the nucleoplasm 15 gold particles/μm^2 for wild-type and 19 gold particles/μm^2 for *rlp7-1* at 37°C. Moreover, the density of the gold in the nucleolus is 99 particles/μm^2 in wild-type cells and 207

Table I. **Yeast strains**

Strain name	Genotype	Origin
RS453a	MATa, *ade2, leu2, ura3, his3, trp1*	Hurt et al., 1999
FY23	MATa, *ura3, trp1, leu2*	derived from S288C
FY86	MATα, *ura3, his3, leu2*	derived from S288C
rix9-1	MATa, *ura3, his3, leu2, rix9-1*	isolated from ts collection (Amberg et al., 1992)
rlp7-1	MATa, *ura3, his3, leu2, trp1, rlp7-1*	Offspring of *rix9-1* original x FY86
Rlp7p-GFP	MATa, *ura3, trp1, his3, leu2, RLP7-GFP::KANMX4*	Offspring of FY23 x FY86
Rlp7p-ProtA	MATa, *ura3, trp1, his3, leu2, RLP7-ProtA::TRP1*	Offspring of FY23 x FY86
noc2-1	MATα, *ura3, his3, leu2, noc2-1*	Milkereit et al., 2001
rix7-1	MATa, *ura3, trp1, his3, leu2, rix7-1*	Gadal et al., 2001
rpl10-1 (or *rix5-1*)	MATα, *ura3, his3, leu2, rpl10-1*	Gadal et al., 2001
BMA64-1b	MATα, *leu2, his3, trp1, ade2, ura3*	Galy et al., 1999
BMA64-1a	MATa, *leu2, his3, trp1, ade2, ura3*	Galy et al., 1999
Rlp7p-CFP	MATa, *leu2, his3, trp1, ade2, ura3, RLP7-CFP::HIS3MX4*	derived from BMA64-1a
CFP-Nop1p	MATa, *leu2, his3, trp1, ade2, ura3 + pUN100-CFP-NOP1*	derived from BMA64-1a
YFP-Nop1p	MATα, *leu2, his3, trp1, ade2, ura3 + pUN100-YFP-NOP1*	derived from BMA64-1b
Gar1p-YFP	MATα, *leu2, his3, trp1, ade2, ura3, GAR1-YFP::TRP1*	derived from BMA64-1b
Gar1p-CFP	MATa, *leu2, his3, trp1, ade2, ura3, GAR1-CFP::HIS3MX4*	derived from BMA64-1a
Nug2p-YFP	MATα, *leu2, his3, trp1, ade2, ura3, NUG2-YFP::TRP1*	derived from BMA64-1b

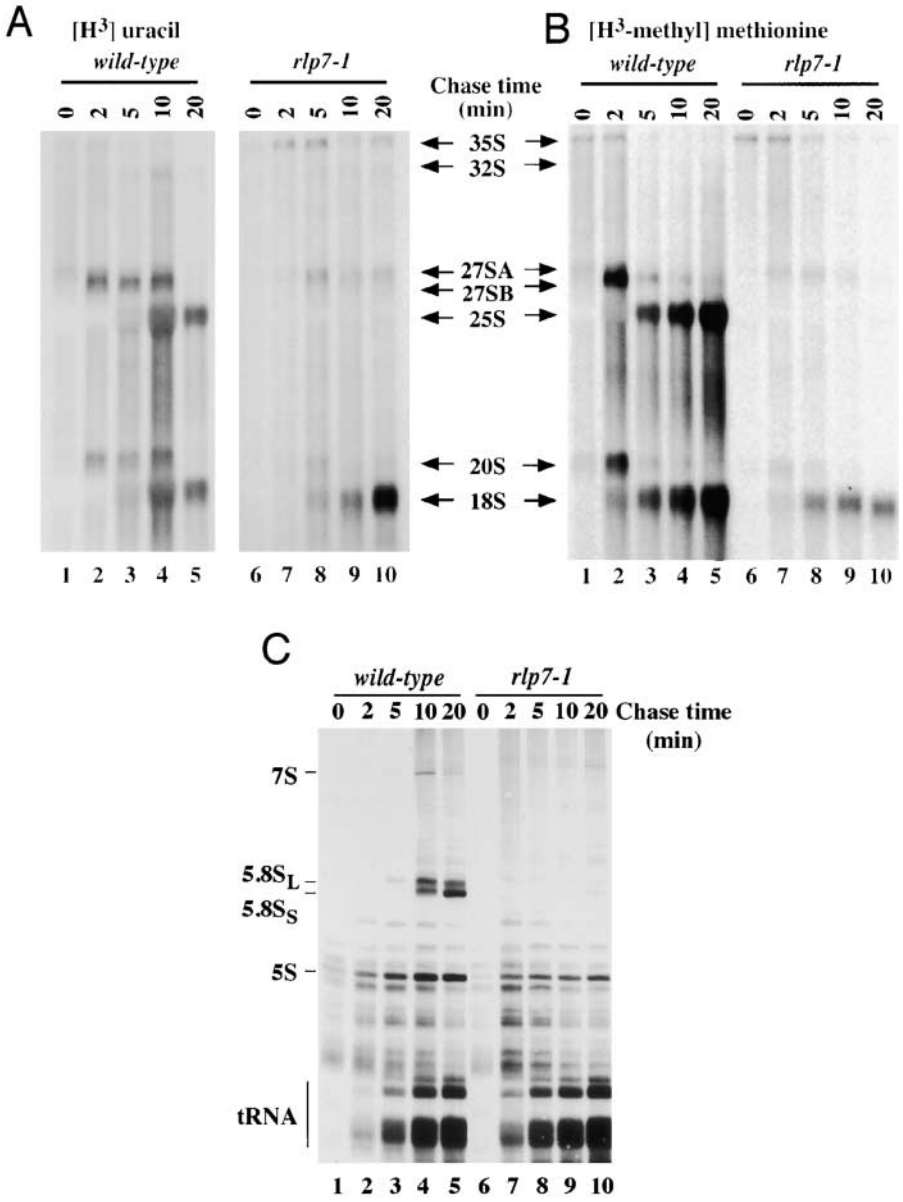

Figure 6. **Pulse-chase analysis of pre-rRNA processing in the *rlp7-1* strain.** Wild-type (lanes 1–5) and *rlp7-1* (lanes 6–10) strains were labelled with [H^3]-uracil for one min or with [H^3-methyl]-methionine for 2 min, and then chased with unlabeled uracil (A) and (C) or methionine (B) for the times indicated.

particles/μm^2 in the *rlp7-1* ts mutant at 37°C. Thus, accumulating pre-rRNAs did not appear to move to the nucleoplasm, but remained confined in the nucleolus. Similar observations were made by FISH with oligonucleotidic probes complementary to the ITS2 (unpublished data). These results are consistent with the localization of Rpl25p-eGFP in the nucleolus at 37°C, and with a defect in 27S pre-rRNA processing.

Rlp7p is localized in the GC of the nucleolus

Rlp7p-GFP was expressed as a construct integrated at the *RLP7* gene locus to avoid overexpression. To confirm that Rlp7p concentrates in the nucleolus as previously shown (Dunbar et al., 2000), it was coexpressed with the nucleolar marker DsRed-Nop1p (Gadal et al., 2001). As expected, the DsRed-Nop1 exhibits a crescent-like staining close to the nuclear periphery, which does not overlap with the DNA staining (Fig. 8 A). However, the fluorescence signal of Rlp7p-GFP, although concentrated in the nucleolus, did not fully overlap with the fluorescence signal of DsRed-Nop1p (Fig. 8 A). This suggests that Rlp7p and Nop1p are nucleolar components, but located in different subnucleolar compartments. To further substantiate this finding, not only Rlp7p and Nop1p, but also additional nucleolar markers, Gar1p as a DFC component (Henras et al., 1998) and Nug2p, which associates with late 60S preribosomes (Bassler et al., 2001), were tagged with spectral variants of GFP (YFP and CFP, respectively), and colocalization was determined by double fluorescence microscopy. Similar to the data shown above, YFP-Nop1p and Rlp7p-CFP expressed in the same strain (for construction of strains, see Materials and methods; Table I) do not reside in the same subnucleolar compartment (Fig. 8 B). Similarly, the Nug2p-YFP and CFP-Nop1p labeling do not overlap (Fig. 8 B). In contrast, Gar1p-YFP and CFP-Nop1p colocalize within the nucleolus (Fig. 8 B), supporting the previous conclusions that both

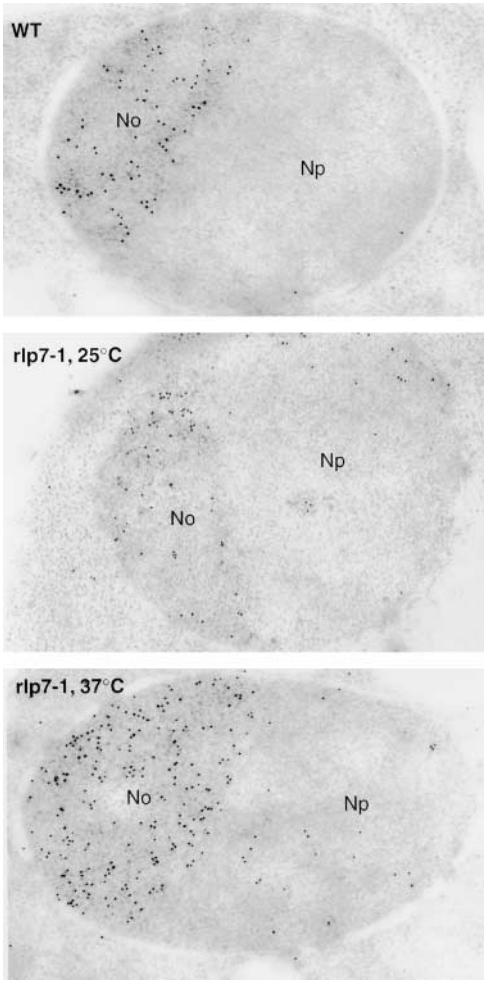

Figure 7. **Ultrastructural localization of pre-60S particles using a ITS2-specific probe in *rlp7-1* cells.** Wild-type and *rlp7-1*cells grown at 25 or at 37°C for 4 h were cryofixated and cryoembedded in LR white resin. ITS2 containing pre-rRNAs were detected with a riboprobe conjugated to biotin.

proteins are DFC components. In contrast, Nug2p-YFP and CFP-Gar1p do not fully overlap (Fig. 8 B), whereas Rlp7p-CFP and Nug2-YFP colocalize within the yeast nucleolus (Fig. 8 B). Moreover, Nug2p-YFP can be also detected in the nucleoplasm, consistent with a role in nuclear export (Bassler et al., 2001), but Rlp7-CFP is restricted to the nucleolar region (Fig. 8 B). Thus, the DFC marker proteins Nop1p and Gar1p colocalize in the yeast nucleolus, whereas Rlp7p and Nug2p also colocalize, but are adjacent to the DFC.

To identify at the ultrastructural level the nucleolar subcompartment in which Rlp7p resides, Nop1p and Rlp7p were immunolocalized on ultrathin sections obtained after high-pressure cryofixation, cryosubstitution, and cryoembedding (Fig. 9). The presence of nucleolar subdomains in *S. cerevisiae* was clearly established by electron microscopy on cells prepared by ultrafast freezing and cryosubstitution in the presence of osmium tetroxide (Léger-Silvestre et al., 1999). Under these conditions, the DFC appeared as a region of high electron density. Here, osmium tetroxide was omitted during cryosubstitution in order to preserve the epitopes on proteins and immunolocalize Nop1p, a marker of the DFC, and Rlp7p-ProtA. In this case, the subnucleolar regions display less contrast. That Rlp7p and Nop1p are differentially located within the nucleolus is confirmed by double labeling experiments in which the two proteins are detected with gold particles of two sizes (Fig. 9). Thus, immuno-EM showed that Rlp7p and Nop1p are not located in the same nucleolar subregions, which explains the data obtained by fluorescence microscopy. We conclude that Rlp7p is associated with pre-60S particles in the nucleolar GC, and is the first identified processing factor to be so localized.

Discussion

Here we report that the *rix9-1* (*rlp7-1*) allele is a mutation in the essential gene *RLP7*. Rlp7p is a nucleolar protein concentrated in the GC and is associated with ribosomal precursors. The *rlp7-1* mutation results in a single phenylalanine$_{176}$ to serine change in Rlp7p, which leads to a ts-lethal phenotype, nucleolar accumulation of an Rpl25p-eGFP reporter construct, and inhibition of pre-rRNA processing.

Subnucleolar structures have long been identified by EM and are the subject of a vast body of research (for review see Shaw and Jordan, 1995; Scheer and Hock, 1999). However, the relationship between nucleolar structures and the steps in ribosome synthesis are not well established. Transcription of the rRNA is likely to occur in the FCs or at the interface between the FCs and the DF). The FCs contain RNA polymerase I and transcription factors, whereas the DFC contains processing factors including fibrillarin (Nop1p in yeast) (Benavente et al., 1988; Pierron et al., 1989; Ochs and Smetana, 1991; Puvion-Dutilleul et al., 1991; Thiry and Goessens, 1992; Léger-Silvestre et al., 1999), which is associated with the box C/D snoRNAs, including U3, that are involved in early pre-rRNA processing and modification steps. In contrast to the FCs and DFC, very little is known about molecular markers for the GC, where late assembly and processing reactions are believed to occur. As an example, ribocharin, which is a nuclear 40-kD protein, was reported to specifically associate with the GC of the nucleolus and with a nucleoplasmic 65S particles (Hügle et al., 1985). Here we identify Rlp7p as a specific GC marker in yeast. Previously, Rlp7p was shown to be present in three different pre-60S particles (Fig. 10; Bassler et al., 2001; Harnpicharnchai et al., 2001; Saveanu et al., 2001; Fatica et al., 2002), indicating that each of these are concentrated in the GC. The 90S preribosomes contain the 35S pre-rRNA and are strongly predicted to be associated with the box C/D snoRNAs that direct the 35S pre-rRNA 2′-*O*-methylation. Therefore, the localization of the 2′-*O*-methylase, Nop1p/fibrillarin, to the DFC is good evidence for the localization of the 90S preribosomes to this region. Nop1p is not associated with the characterized pre-60S particles, and we predict that release from the DFC coincides with the formation of an early pre-60S particle, e.g., the pre-60S E_1 complex shown in Fig. 10. Maturation through pre-60S E_2 and pre-60S M is proposed to occur in the GC, with release of a complex located on the pathway between pre-60S M and pre-60S L from the GC into the nucleoplasm.

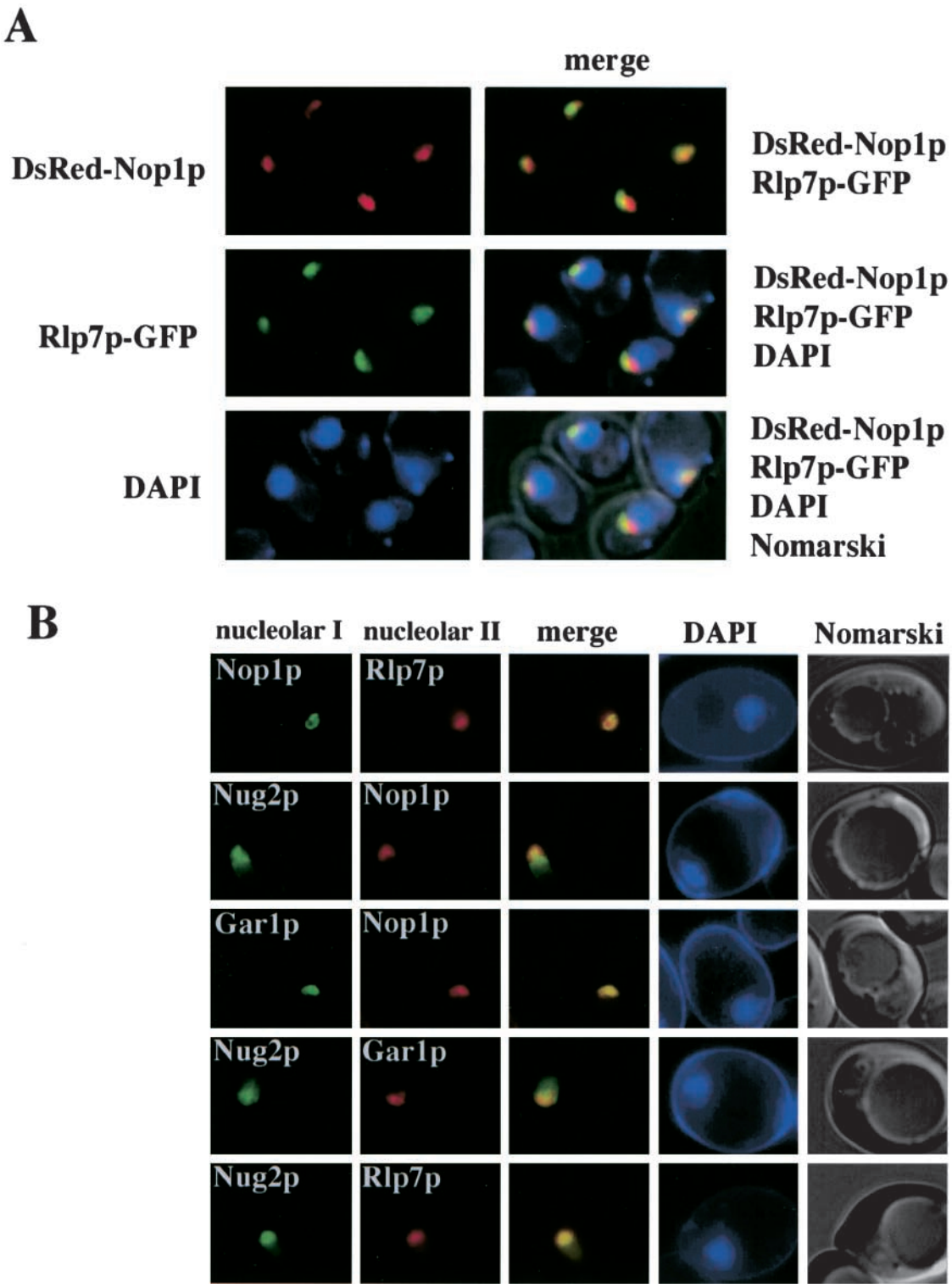

Figure 8. **Rlp7p is located in the subnucleolar GC compartment.** (A) Rlp7p-GFP is nucleolar but does not fully overlap with Nop1p. Strain Rlp7p-GFP harboring a plasmid expressing DsRed-Nop1p was grown at 23°C to OD_{600nm} of 0.5. The DNA-staining dye DAPI was added to the cells 5 min before microscopic inspection of the GFP signal, DsRed, and DAPI in the fluorescence microscope. Cells were also visualized by Nomarski imaging. Shown are also merged pictures as indicated. (B) Rlp7p colocalizes with Nug2p, but does not overlap with the DFC markers Gar1p and Nop1p. Diploid strains, which were constructed by mating of haploid strains (Table I), expressed the following combinations of spectral GFP variants: YFP-Nop1p/Rlp7p-CFP; Nug2p-YFP/CFP-Nop1p; Gar1p-YFP/CFP-Nop1p; Nug2p-YFP/Gar1p-CFP; and Nug2p-YFP/Rlp7p-CFP. Cells grown at 30°C were harvested in the exponential growth phase (OD_{600nm} 0.5), before the YFP (green; nucleolar I), CFP (red; nucleolar II) and Hoechst (blue) fluorescence signals were detected by fluorescence microscopy. The green and red signals were also merged (merge). The DNA staining and Nomarski pictures are also shown.

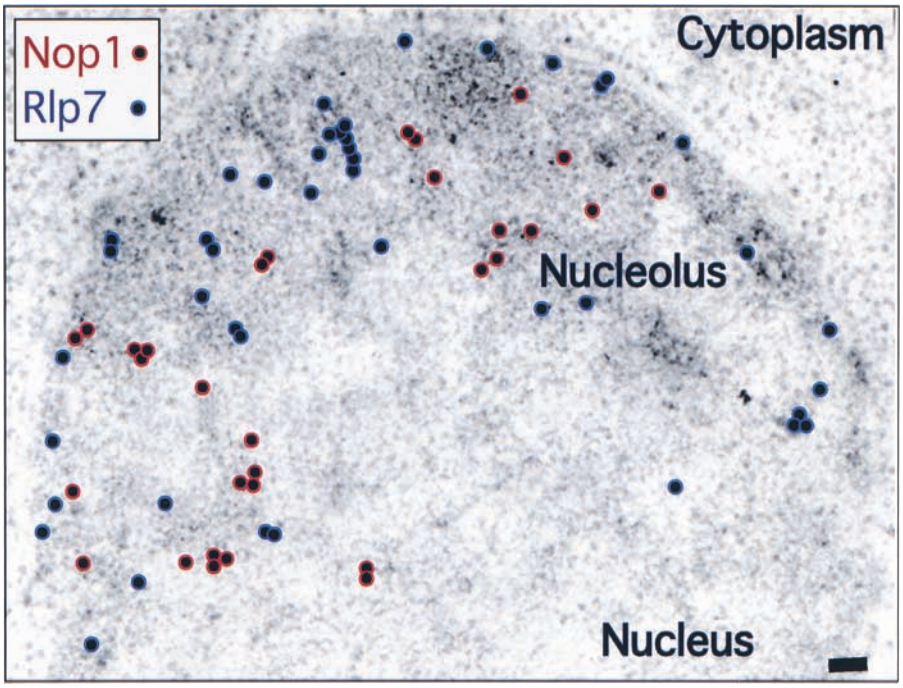

Figure 9. **Immunolocalization of Nop1p and Rlp7p-ProtA by EM.** Exponentially growing cells were prepared for EM by high-pressure ultrafast freezing and cryoembedding in LR White resin. Nop1p and Rlp7p-Prot A were detected by immunogold labeling with an anti-Nop1 monoclonal antibody and a polyclonal anti–protein A antibody, respectively. Nop1p and Rlp7p-Prot A are codetected with gold particles of 5 (labeled with a red circle) and 10 nm (labeled with a blue circle) in diameter, respectively. Bar, 100 nm.

Rlp7p is required for efficient processing from site A_3 to B_{1S}, the 5′ end of the major form of the 5.8S rRNA, and for pre-rRNA cleavage at site C_2 in ITS2, which separates the precursors to the 5.8S and 25S rRNAs, and is also required for 60S subunit export. It seems likely that these activities take place in different preribosomal particles. Processing from A_3 to B_{1S} is believed to occur within the pre-60S E_1 complex, cleavage at site C2 within pre-60S E_2 and acquisition of export competence within pre-60S M (Fatica et al., 2001; Offinger et al., 2002). Another characterized protein, Nop7p, is also found in the same complexes as Rlp7p (Bassler et al., 2001; Harnpicharnchai et al., 2001; Fatica et al., 2002). Depletion of Nop7p also resulted in the inhibition of processing from A_3 to B_{1S} and nuclear accumulation of Rpl25p-GFP, suggesting that it performs functions related to Rlp7p within the pre-60S E_1 and pre-60S M complexes. In contrast, Nop7p depletion did not prevent C_2 cleavage, but expression of Rpl25-GFP was lethal in cells lacking Nop7p. Rpl25p is likely to associate with the pre-60S E_2 complex (Harnpicharnchai et al., 2001; Fatica et al., 2002), indicating that Nop7p plays some role in subunit assembly within this complex but, unlike Rlp7p, is not required for C_2 cleavage within pre-60S E_2.

The inhibition of cleavage at site C_2 is a relatively specific phenotype, as several other mutations that inhibit 5.8S and 25S synthesis did not prevent C_2 cleavage. These include the mutations *noc2-1*, *rpl10-1*, and *rix7-1*, which inhibit export of the 60S preribosomes, suggesting that the inhibition of C_2 cleavage in the *rlp7-1* strain is not the direct cause of the transport defect.

While this work was in progress, Dunbar et al. (2000) reported an analysis of the function of Rlp7p in pre-rRNA processing using a depletion approach. Rlp7p depletion was shown to inhibit 5.8S and 25S rRNA production, consistent with our observations.

Rlp7p is highly homologous to ribosomal protein L7, suggesting that they may compete for the same binding site on the rRNA. Because the 3′ end of the 5.8S and the 5′ end of the 25S rRNA are distant from the L7 binding site on the mature ribosome, it is unlikely that Rlp7p binds the ribosome close to the C2 cleavage site (Spahn et al., 2001). Following its function in pre-rRNA cleavage, Rlp7p could be dissociated from the rRNA by the binding of Rpl7p, poten-

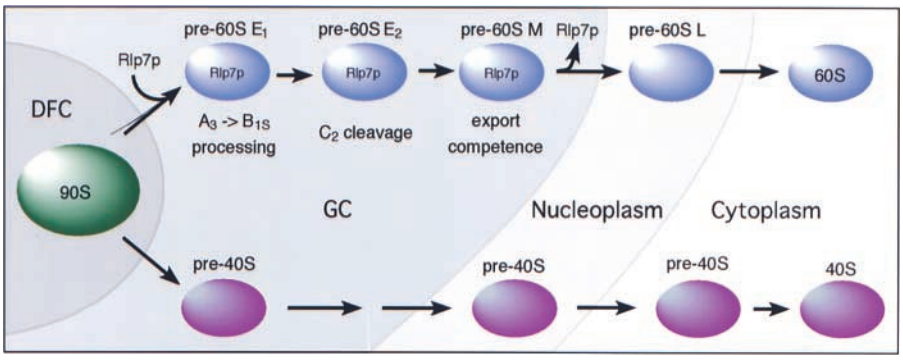

Figure 10. **Model of Rlp7p function during nucleolar pre-rRNA processing and ribosome assembly.** See text for details.

tially ensuring the correct succession of processing and assembly events. This strategy may be common in ribosome biogenesis, as three other known pre-rRNA–processing and –assembly factors show high similarity to proteins involved in translation. The U3 snoRNP protein Imp3p, which functions in 40S subunit synthesis, is homologous to the 40S protein Rps9p (Dunbar et al., 2000), the 60S preribosome components Yhr052p and Rlp24p are homologous to Rpl1p and Rpl24p, respectively (Bassler et al., 2001; Saveanu et al., 2001), and Efl1p is homologous to the translation elongation factor EF-2 (Senger et al., 2001).

This finding has potential relevance for the evolution of ribosome biogenesis. Ribosome biogenesis in prokaryotic cells occurs in a single cell compartment, whereas the synthesis of eukaryotic ribosomes involves a succession of transport events from the nucleolus to the cytoplasm. We suggest that intracellular transport systems for preribosomes initially recognized ribosomal proteins. During evolution, duplication of these components led to the separation of the ribosomal proteins and homologous proteins that bind to the same sequence in preribosomes. Replacement of the preribosomal protein with the ribosomal protein could act as a signal for release of the preribosomal particle from a specific region. In the simplest model, Rlp7p might be physically associated with preribosomal particles during their assemblage in the GC. By analogy, Imp3p and perhaps the U3 snoRNP might be required for the retention of the 90S preribosomes in the DFC, whereas the replacement of Efl1p by EF-2 might signal arrival of the subunits in the cytoplasm (Senger et al., 2001; unpublished data).

In summary, using a genetic screen to identify novel components required for the export of the large ribosomal particle, we identified a mutation in Rlp7p. We have shown that Rlp7p is enriched in a subcompartment of the nucleolus, the GC. Rlp7p is required for the C_2 cleavage that occurs within a ribosomal precursor particle. Rlp7p belongs to the increasing family of maturation proteins with high homology to a component of the translation machinery. Therefore, we suggest that this family of proteins could allow retention of the premature particles in specific areas of the nucleus during their maturation. Using this strategy eukaryotic cells could achieve precise coupling between ribosome maturation and its nuclear export.

Materials and methods

Yeast strains, DNA manipulation, and microbiological techniques

Yeast strains used in this study are listed in Table I. Microbiological techniques, plasmid transformation and recovery, mating, sporulation of diploid, and tetrad analysis were performed essentially as described (Santos-Rosa et al., 1998). DNA manipulation was performed according to (Maniatis et al., 1982).

Plasmid constructions

Plasmids pUN100-DsRed-Nop1p, pRS314-DsRed-Nop1p, pRS316-Rpl25p-eGFP, pFA6a-(2*ProtA-TEV)-TRP1, and pFA6a-GFP(S65T)-kanMX6 were described previously (Longtine, 1998; Gadal et al., 2001). pFA6-YFP-TRP1, pFA6-CFP-TRP1, pFA6-YFP-HIS3MX6, and pFA6-CFP-HIS3MX6 are derivative of pFA6a-GFP(S65T)-HIS3MX6 and pFA6-GFP-TRP1 (Longtine et al., 1998), where the *Pac1-Asc1* fragment, bearing the GFP-coding sequence, was PCR exchanged with the corresponding eYFP and eCFP spectral variant of GFP, using vectors pECFP-C1 and pEYFP-C1 from CLONTECH Laboratories, Inc. Plasmids pUN100-YFP-Nop1p and pUN100-CFP-Nop1p are derivative of pUN100-DsRed-Nop1p where the *SphI-SphI* fragment, bearing the GFP-coding sequence, was PCR exchanged with the corresponding eYFP and eCFP spectral variant of GFP, using vectors pECFP-C1 and pEYFP-C1 from CLONTECH Laboratories, Inc.

Strain constructions

Genomic integration of GFP in frame with *RLP7* was obtained as described previously (Longtine et al., 1998). Genomic integration of ProtA in frame with *RLP7*, *YFP*, and *CFP* in frame with *RLP7, GAR1*, and *NUG2* were done in the same way, but using, respectively, the pFA6a-(2*ProtA-TEV)-TRP1, pFA6-YFP-TRP1, pFA6-CFP-TRP1, pFA6-YFP-HIS3MX6, and pFA6-CFP-HIS3MX6 vectors.

Cloning of RIX9/RLP7

A yeast genomic library in an *LEU2*-containing *ARS/CEN* plasmid (Gautier et al., 1997) was transformed into the *rix9-1* strain. From colonies growing at the restrictive temperature (37°C), plasmid p*RIX9* with a genomic insert was isolated. The complementing plasmid contained the *RLP7* gene. p*RLP7* harboring only the *RLP7* gene was cloned and shown to complement the ts growth defect of the *rix9-1* mutant.

Pulse-chase and Northern analysis of rRNA

Pulse-chase labelling of rRNA, primer extension, and analysis of rRNA processing by Northern hybridization was performed as described (Tollervey, 1987; Tollervey et al., 1993). Oligonucleotides used were: 003, TGT TAC CTC TGG GCC C; 004, CGG TTT TAA TTG TCC TA; 007, CTC CGC TTA TTG ATA TGC; 008, CAT GGC TTA ATC TTT GAG AC; 013, GGC CAG CAA TTT CAA GTT A; 017, GCG TTG TTC ATC GAT GC; 020, TGA GAA GGA AAT GAC GCT; 219, GAA GCG CCA TCT AGA TG, and 5′ A_0L GGT CTC TCT GCT GCC GG.

Fluorescence microscopy

pRS315-Rpl25p-eGFP or pRS316-Rpl25p-eGFP was introduced into yeast cells by transformation and selected on SDC-leu or SDC-ura medium, respectively. Individual transformants were grown in liquid SDC-leu medium at 23°C to OD(600 nm) of ~1, before shift to 37°C in liquid YPD medium. After centrifugation, cells were resuspended in water, mounted on a slide, and observed in the fluorescence microscope. In vivo, the GFP signal was examined in the FITC fluorescent channel; the DsRed used in fusion with Nop1p was examined in the rhodamine channel of a Zeiss Axioskop fluorescence microscope, and pictures were obtained with a Xillix Microimager CCD camera. Digital pictures were processed by software program Open lab (Improvision) and Adobe Photoshop® (v. 4.0.1).

Fluorescence microscopy of green fluorescent protein spectral variants was done on exponentially growing cells, which were washed in water and stained with Hoechst 33352 (5 ng/μl) for 5 min. Samples were examined using a Leica DMRXA fluorescence microscope. Fluorescent signals were collected with single-band pass filters for excitation of YFP (XF104; Omega Optical), CFP (XF114-2; Omega optical), and Hoechst (Leica). Images were acquired with a Hamamatsu C4742-95 cooled CCD camera controlled by the Openlab® software (Improvision) and processed with the Adobe Photoshop® software.

EM

Protein A–tagged Rlp7p strains were prepared for EM using high-pressure freezing. After preembedding in low–melting point agarose, cells moistened with the freezing medium (1-hexadecene) were loaded into specimen holder and frozen with liquid nitrogen under high pressure using the EM Pact system (Leica SA). The frozen samples were then transferred in 0.4% uranyl acetate in absolute acetone. Substitution fixation was carried out at −90°C for 3 d. The specimen were gradually transferred to −20°C, washed successively with absolute acetone and absolute ethanol at −20°C, infiltrated, and embedded with LR White resin at this temperature. For immunolocalization of the protein A–tagged Rlp7p, we used a polyclonal anti–protein A antibody from Sigma-Aldrich. This antibody was labeled with gold-conjugated goat anti–rabbit IgG (British Bio-Cell). No nuclear labelling was detected when immunolocalization was performed on cells devoid of Protein A–tagged protein, or when the primary antibodies were omitted. Nop1*p* was detected using a monoclonal antibody from Dr. J. Aris (University of Florida, Gainesville, FL) and goat anti–mouse IgG gold–conjugated. In situ hybridization of pre-rRNAs using an ITS2-specific riboprobe was performed as previously described (Gleizes et al., 2001). The probe was generated by in vitro transcription in the presence of UTP-biotin and detected on sections with anti-biotin antibodies conjugated to 10-nm gold particles.

Miscellaneous

SDS-PAGE and Western blot analysis were performed according to (Siniossoglou et al., 1996), and isolation of ribosomes under low-salt conditions by sucrose gradient centrifugation as described in (Tollervey et al., 1993). Whole-cell lysates and fractions from the sucrose gradients were separated by SDS-PAGE and analysed by Western blotting using the indicated antibodies.

E.C. Hurt is recipient of grants from the Deutsche Forschungsgemeinschaft (Schwerpunktprogramm "Funktionelle Architektur des Zellkerns"), E. Petfalski and D. Tollervey were funded by the Wellcome Trust, and O. Gadal was a holder of a Human Frontiers Science Program fellowship. P.E. Gleizes and N. Gas are supported by a grant from the Association pour la Recherche contre le Cancer.

Submitted: 9 November 2001
Revised: 17 April 2002
Accepted: 18 April 2002

References

Amberg, D.C., A.L. Goldstein, and C.N. Cole. 1992. Isolation and characterization of *RAT1*: an essential gene of *Saccharomyces cerevisiae* required for the efficient nucleocytoplasmic trafficking of mRNA. *Genes Dev.* 6:1173–1189.

Bassler, J., P. Grandi, O. Gadal, T. Lessmann, D. Tollervey, J. Lechner, and E.C. Hurt. 2001. Identification of a 60S preribosomal particle that is closely linked to nuclear export. *Mol. Cell.* 8:517–529.

Benavente, R., G. Reimer, K.M. Rose, B. Hügle-Dörr, and U. Scheer. 1988. Nucleolar changes after microinjection of antibodies to RNA polymerase I into the nucleus of mammalian cells. *Chromosoma.* 97:115–123.

Dunbar, D.A., F. Dragon, S.J. Lee, and S.J. Baserga. 2000. A nucleolar protein related to ribosomal protein L7 is required for an early step in large ribosomal subunit biogenesis. *Proc. Natl. Acad. Sci. USA.* 97:13027–13032.

Fatica, A., A.D. Cronshaw, M. Dlakic, and D. Tollervey. 2002. Ssf1p prevents premature processing of an early pre60S ribosomal particle. *Mol. Cell.* 9:341–351.

Gadal, O., D. Strauss, J. Kessl, B. Trumpower, D. Tollervey, and E. Hurt. 2001. Nuclear export of 60S ribosomal subunits depends on Xpo1p and requires a NES-containing factor Nmd3p that associates with the large subunit protein Rpl10p. *Mol. Cell. Biol.* 21:3405–3415.

Galy, V., J. Olivo-Martin, H. Scherthan, V. Doye, N. Rascalou, and U. Nehrbass. 2000. Nuclear pore complexes in the organization of silent telomeric chromatin. *Nature.* 403:108–112.

Gautier, T., T. Bergès, D. Tollervey, and E. Hurt. 1997. Nucleolar KKE/D repeat proteins Nop56p and Nop58p interact with Nop1p and are required for ribosome biogenesis. *Mol. Cell. Biol.* 17:7088–7098.

Gleizes, P.E., J. Noaillac-Depeyre, I. Leger-Silvestre, F. Teulieres, J.Y. Dauxois, D. Pommet, M.C. Azum-Gelade, and N. Gas. 2001. Ultrastructural localization of rRNA shows defective nuclear export of preribosomes in mutants of the Nup82p complex. *J. Cell Biol.* 155:923–936.

Harnpicharnchai, P., J. Jakovljevic, E. Horsey, T. Miles, J. Roman, M. Rout, D. Meagher, B. Imai, Y. Guo, C.J. Brame, J. Shabanowitz, D.F. Hunt, and J.L. Woolford. 2001. Composition and functional characterization of yeast 66s ribosome assembly intermediates. *Mol. Cell.* 8:505–515.

Henras, A., Y. Henry, C. Bousquet-Antonelli, J. Noaillac-Depeyre, J.P. Gélugne, and M. Caizergues-Ferrer. 1998. Nhp2p and Nop10p are essential for the function of H/ACA snoRNPs. *EMBO J.* 17:7078–7090.

Hügle, B., U. Scheer, and W.W. Franke. 1985. Ribocharin: a nuclear M_r 40.000 protein specific to precursor particles of large ribosomal subunit. *Cell.* 41: 615–627.

Kressler, D., P. Linder, and J. De La Cruz. 1999. Protein trans-acting factors involved in ribsome biogenesis in *Saccharomyces cerevisiae*. *Mol. Cell. Biol.* 19: 7897–7912.

Lalo, D., S. Mariotte, and P. Thuriaux. 1993. Two distinct yeast proteins are related to the mammalian ribosomal polypeptide L7. *Yeast* 9:1085–1091.

Léger-Silvestre, I., S. Trumtel, J. Noaillac-Depeyre, and N. Gas. 1999. Functional compartmentalization of the nucleus in the budding yeast *Saccharomyces cerevisiae*. *Chromosoma.* 108:103–113.

Longtine, M.S., A. McKenzie, D.J. Demarini, N.G. Shah, A. Wach, A. Brachat, P. Philippsen, and J.R. Pringle. 1998. Additional modules for versatile and economical PCR-based gene deletion and modification in *Saccharomyces cerevisiae*. *Yeast* 10:953–961.

Maniatis, T., E.T. Fritsch, and J. Sambrook. 1982. Molecular Cloning: A Laboratory Manual. Cold Spring Harbor Laboratory Press, Cold Spring Harbor, NY.

Milkereit, P., O. Gadal, A. Podtelejnikov, S. Trumtel, N. Gas, E. Petfalski, D. Tollervey, M. Mann, E. Hurt, and H. Tschochner. 2001. Maturation of ribosomes requires Noc proteins and is coupled to transport from the nucleolus to the nucleoplasm. *Cell.* 105:499–509.

Ochs, R.L., and K. Smetana. 1991. Detection of fibrillarin in nucleolar remnants and the nucleolar matrix. *Exp.Cell Res.* 197:183–190.

Oeffinger, M., A. Lueng, A. Lamond, and D. Tollervey. 2002. Yeast Pescadillo is required for multiple activities during 60S ribosomal subunit synthesis. *RNA*. 8:626–636.

Pierron, G., J. Pedron, M. Schelling, and M. Christensen. 1989. Immunoelectron microscopic localization of the nucleolar protein B-36 (fibrillarin) during the cell cycle of Physarum polycephalum. *Biol. Cell.* 65:119–126.

Puvion-Dutilleul, F., S. Mazan, M. Nicoloso, M.E. Christensen, and J.-P. Bachellerie. 1991. Localization of U3 RNA molecules in nucleoli of HeLa and mouse 3T3 cells by high resolution in situ hybridization. *Eur. J. Cell Biol.* 56:178–186.

Santos-Rosa, H., H. Moreno, G. Simos, A. Segref, B. Fahrenkrog, N. Panté, and E. Hurt. 1998. Nuclear mRNA export requires complex formation between Mex67p and Mtr2p at the nuclear pores. *Mol. Cell. Biol.* 18:6826–6838.

Saveanu, C., D. Bienvenu, A. Namane, P.E. Gleizes, N. Gas, A. Jacquier, and M. Fromont-Racine. 2001. Nog2p, a putative GTPase associated with pre60S subunits and required for late 60S maturation steps. *EMBO J.* 20:6475–6484.

Scheer, U., and R. Hock. 1999. Structure and function of the nucleolus. *Curr. Opin. Cell Biol.* 11:385–390.

Senger, B., D.L.J. Lafontaine, J.-S. Graindorge, O. Gadal, A. Camasses, A. Sanni, J.-M. Garnier, M. Breitenbach, E.C. Hurt, and F. Fasiolo. 2001. The nucle(ol)ar Tif6p and Efl1p, a novel EF-2 like GTPase, are required for a late cytoplasmic step of ribosome synthesis. *Mol. Cell.* 8:1363–1373.

Shaw, P.J., and E.G. Jordan. 1995. The nucleolus. *Annu. Rev. Cell Biol.* 11:93–121.

Shuai, K., and J.R. Warner. 1991. A temperature sensitive mutant of *Saccharomyces cerevisiae* defective in prerRNA processing. *Nucleic Acids Res.* 19:5059–5064.

Sillevis-Smitt, W.W., J.M. Vlak, I. Molenaar, and T.H. Rozijn. 1973. Nucleolar function of the dense crescent in the yeast nucleus. *Exp. Cell Res.* 80:313–321.

Siniossoglou, S., C. Wimmer, M. Rieger, V. Doye, H. Tekotte, C. Weise, S. Emig, A. Segref, and E.C. Hurt. 1996. A novel complex of nucleoporins, which includes Sec13p and a Sec13p homologue, is essential for normal nuclear pores. *Cell.* 84:265–275.

Spahn, C.M., R. Beckmann, N. Eswar, P.A. Penczek, A. Sali, G. Blobel, and J. Frank. 2001. Structure of the 80S ribosome from *Saccharomyces cerevisiae*—tRNA-ribosome and subunit-subunit interactions. *Cell.* 107:373–386.

Thiry, M., and G. Goessens. 1992. Where, within the nucleolus, are the rRNA genes located? *Exp. Cell Res.* 200:1–4.

Tollervey, D. 1987. A yeast small nuclear RNA is required for normal processing of preribosomal RNA. *EMBO J.* 6: 4169–4175.

Tollervey, D., H. Lehtonen, R.P. Jansen, H. Kern, and E.C. Hurt. 1993. Temperature-sensitive mutations demonstrate roles for yeast fibrillarin in prerRNA processing, prerRNA methylation, and ribosome assembly. *Cell.* 72:443–457.

Trapman, J., J. Retel, and R.J. Planta. 1975. Ribosomal precursor particles from yeast. *Exp.Cell Res.* 90:95–104.

Venema, J., and D. Tollervey. 1999. Ribosome synthesis in *Saccharomyces cerevisiae*. *Annu. Rev. Genet*. 33:261–311.

von Mikecz, A., E. Neu, U. Krawinkel, and P. Hemmerich. 1999. Human ribosomal protein L7 carries two nucleic acid-binding domains with distinct specificities. *Biochem. Biophys. Res. Commun.* 258:530–536.

Warner, J.R. 1999. The economics of ribosome biosynthesis in yeast. *Trends Biochem. Sci.* 24:437–440.

Woolford, J.L., Jr. 1991. The structure and biogenesis of yeast ribosomes. *Adv. Genet.* 29:63–118.